

Testing Ionospheric influence on Substorm Onset Location

Reham Elhawary¹, Karl Laundal², Jone Peter Reistad³, and Spencer Mark Hatch¹

¹Birkeland Centre for Space Science

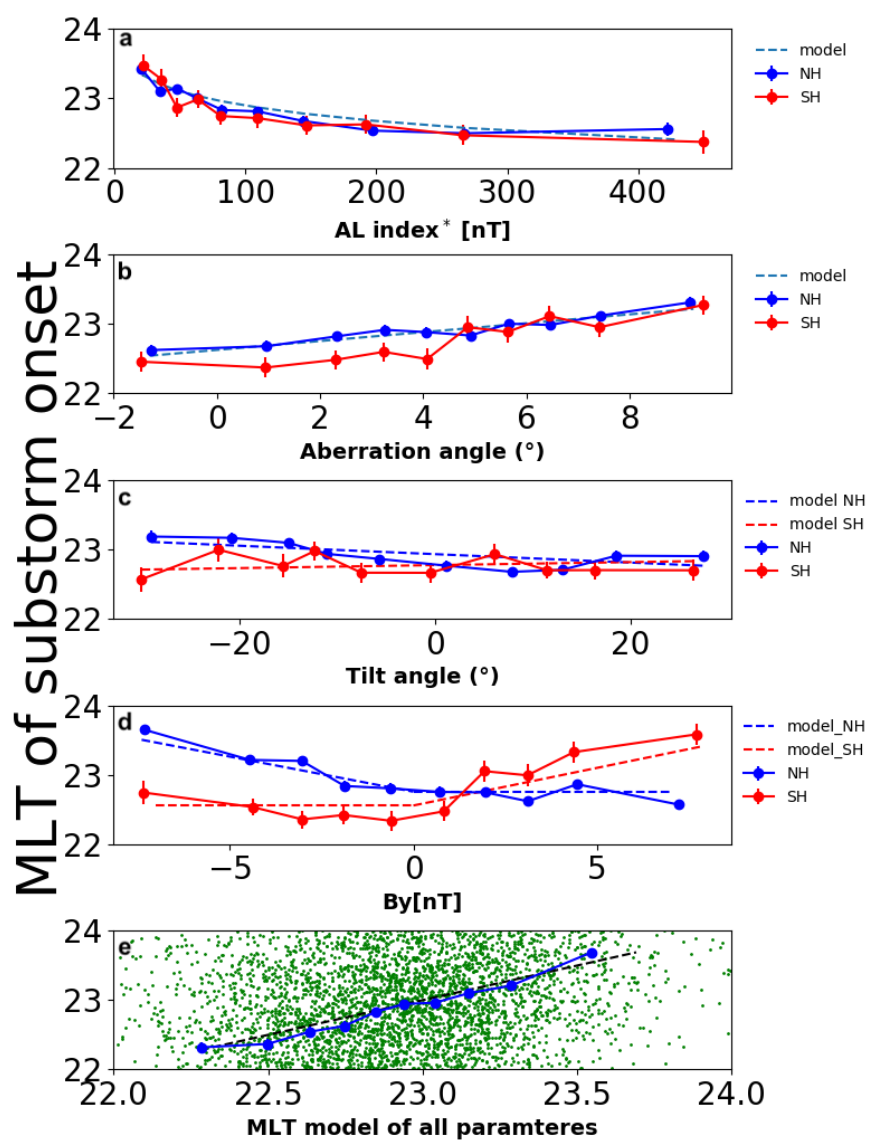
²University in Bergen

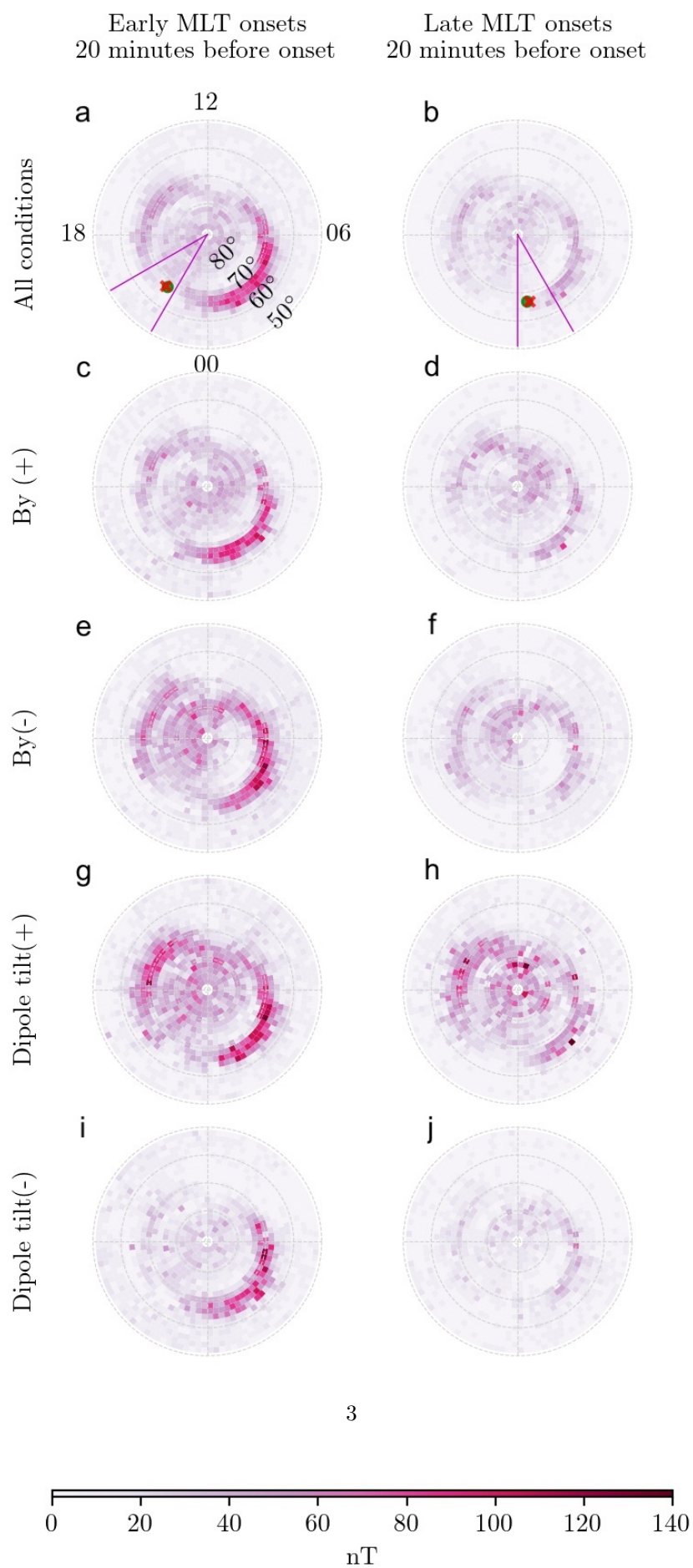
³Birkeland Centre for Space Science, University of Bergen

November 23, 2022

Abstract

Substorm onset location varies over a range of magnetic local times (MLTs) and magnetic latitudes (MLats). Different studies have shown that about 5% of the variation in onset MLT can be explained by variations in interplanetary magnetic field orientation and seasonal variations. Both parameters introduce an azimuthal component to the magnetic field in the magnetosphere such that the projection of the onset MLT in the ionosphere is shifted. Recent studies have suggested that gradients in the ionospheric Hall conductance lead to a duskward shift of the magnetotail dynamics, which could also influence the location of substorm onset. In this paper, we quantify the dependence of the spatial variation of the onset location on the geomagnetic activity level prior to onset. We find that the dependence of onset location on prior conditions is as strong as the dependence on IMF By.





Testing Ionospheric influence on Substorm Onset Location

R. Elhawary¹, K.M. Laundal¹, J.P. Reistad¹, S.M. Hatch¹

¹Birkeland Centre for Space Science, University of Bergen, Bergen, Norway

Key Points:

- Ionospheric conditions prior to substorm onset are different for substorms with an early local time onset vs. late local time onset.
- Substorm onsets tend to occur at earlier local times during geomagnetically active periods than during quiet times.
- We suggest that ionospheric conductance leads to a duskward shift in magnetospheric substorm activity.

Corresponding author: R. Elhawary, reham.elhawary@uib.no

Abstract

Substorm onset location varies over a range of magnetic local times (MLTs) and magnetic latitudes (MLats). Different studies have shown that about 5% of the variation in onset MLT can be explained by variations in interplanetary magnetic field orientation and seasonal variations. Both parameters introduce an azimuthal component to the magnetic field in the magnetosphere such that the projection of the onset MLT in the ionosphere is shifted. Recent studies have suggested that gradients in the ionospheric Hall conductance lead to a duskward shift of the magnetotail dynamics, which could also influence the location of substorm onset. In this paper, we quantify the dependence of the spatial variation of the onset location on the geomagnetic activity level prior to onset. We find that the dependence of onset location on prior conditions is as strong as the dependence on IMF B_y .

Plain Language Summary

Substorms are explosive disturbances in our magnetotail that impact the earth's ionosphere. They happen on average several times per day and as a result of this phenomenon we can see the marvelous aurora. Substorms happen on the nightside of the earth and can take place over a wide range of latitudes and longitudes. In this paper, we show that substorms tend to begin at earlier local times during geomagnetically active times than during quiet times. We interpret this tendency as a sign that ionospheric conditions may play a role in determining where substorms occur.

1 Introduction

Substorms are abrupt global-scale changes in the magnetotail that release the energy stored in the nightside magnetosphere into the two nightside polar ionospheres via field-aligned currents and particle precipitation. Akasofu (1964) defined the substorm in terms of two phases, the expansion phase, and the recovery phase. Later McPherron (1970) defined a third phase of the substorm, the growth phase. The growth phase of the substorm is the period prior to the onset of the expansion phase, typically lasting for 30–60 minutes (Lui, 1991), when kinetic energy in the solar wind is transferred to magnetic energy in the magnetotail. During the expansion phase, the aurora suddenly becomes bright and evolves into a global distribution in typically 10–30 minutes. Finally, a recovery phase can last for more than 2 hours. See, e.g., McPherron & Chu (2016) for a detailed review about the development of the definition of substorms.

Substorms are important events coupling the solar wind-magnetospheric-ionospheric system. S. E. Milan et al. (2010) demonstrated the importance of the substorm as a process by which the magnetosphere releases the opened magnetic flux back to the solar wind through reconnection in the neutral sheet of the tail. Substorms release energy in the magnetotail which reorganizes ionospheric electric field structures and flows. Grocott et al. (2017) showed that the nightside convection morphology is highly dependent on the MLT of the substorm onset.

Global UV images of the aurora have shown that 80% of substorm onsets (i.e., between the 10th and 90th percentile) happen in a ~ 3.2 h wide range of magnetic local time, centered pre-midnight Frey et al. (2004); Liou (2010). Beyond this statistical distribution, the location of substorm onsets remains largely unpredictable. Previous studies have attempted to predict the location of the substorm onset by correlating the MLT and MLAT of the substorm onset with different parameters. For instance, Liou et al. (2001) found that substorms occur at lower latitudes when the IMF B_z component is negative, compared to positive. Gérard et al. (2004) also found a correlation between MLAT of the substorm onset and solar wind dynamic pressure. Both effects may be the result of

relatively more open flux in the magnetosphere, which moves the auroral oval equatorward Milan et al. (2009).

Many other studies have shown that the substorm onset MLT depends on the polarity of IMF B_y rather than IMF B_z (Østgaard et al., 2011, 2004, 2005; Liou & Newell, 2010; Wang et al., 2007). Using the lists of substorm onsets based on global UV imaging by Frey et al. (2004) and Liou (2010), Østgaard et al. (2011) showed that the substorm onset MLT and IMF B_y are correlated. Though the relationship between IMF B_y and substorm onset MLT is statistically significant, IMF B_y only explains 5% of the variation of the substorm onset MLT. Tenfjord et al. (2015) argued that the asymmetric addition of open flux during IMF B_y periods leads to an induced B_y in the magnetosphere, which in turn can lead to changes in the observed projection of the substorm onset on the ionosphere. This projection effect may explain the observed variation of onset location vs IMF B_y . Furthermore, simultaneous observations of substorm onsets in the two hemispheres show that the correlation of the relative shift in MLT with IMF B_y is much higher (Østgaard et al., 2005), consistent with our interpretation that the IMF B_y effect is due to a relative shift between hemispheres (mapping), and not a real shift of the onset location in the magnetosphere. In addition to IMF B_y , the dipole tilt angle may also have a similar effect on the observed onset location in the ionosphere: Due to tail warping associated with nonzero dipole tilt (e.g. Tsyganenko, 1998), a positive dipole tilt angle will project onsets that happen at dusk to earlier (later) local times in the northern (southern) hemisphere. Statistics presented by Liou & Newell (2010) and Østgaard et al. (2011) are consistent with this idea.

The results presented in these previous studies may be completely explained by mapping effects, while the location of the onset in the magnetotail remains unpredictable. The observed shift towards dusk of the typical onset location is similar to the observed distribution of tail reconnection (e.g. Gabrielse et al., 2014). To explain this, Lotko et al. (2014) performed three MHD simulations: In the first simulation, they introduced uniform ionospheric conductance and observed a symmetric magnetotail activity. In the second simulation, they introduced high Hall conductance in the auroral oval and monitored magnetotail activity shifted towards dusk. In the third simulation, they introduced an unrealistic depression in Hall conductance in the auroral oval and monitored magnetotail activity shifted towards dawn. The results of Lotko et al. (2014) suggest that ionospheric feedback influences the duskward shift of tail reconnection and, possibly, substorm onsets. In this paper, we test this idea using observations of substorm onsets, ground magnetic field perturbations, and solar wind conditions.

2 Observations

We use the Frey et al. (2004) and Liou (2010) lists to investigate substorm onsets in this paper. The two lists combined have 6192 substorms in the period 1996–2005, with 4762 substorms observed in the Northern hemisphere and 1430 substorms observed in the Southern hemisphere. To investigate whether the ionospheric state may possibly influence substorm onset location, we used horizontal geomagnetic data from the northern hemisphere. Figure 1 shows maps of the average horizontal magnetic field perturbations (ground B). The colors represent the median ground B perturbations 20 minutes prior to substorm onsets for different conditions of IMF B_y and dipole tilt angle. The ground magnetic field perturbations were obtained from the SuperMAG (Gjerloev, 2012) database and converted to quasi-dipole coordinates (Richmond, 1995; Laundal & Richmond, 2017).

The left column shows onsets observed between 20 and 22 MLT (hereafter “early onsets”) and the right column shows onsets observed between 24 and 02 MLT (“late onsets”), as the distribution of the substorm onsets is centered around 23 MLT Liou & Newell (2010); Gérard et al. (2004). Figures 1a and 1b show the median magnetic field pertur-

bations 20 minutes prior to early and late substorm onsets, respectively. The magenta lines are the boundaries of the onset locations. The red cross \times is the location of the mean onset location while the green circle \bullet is the median. The median MLT of the early (late) subset is 21.47 (0.54). We find that the magnitude of ground B is generally higher during the 20 min preceding early substorm onsets than during the 20 min preceding late substorm onsets.

The separation into early and late onsets biases the distributions of IMF B_y and dipole tilt angle since we know that these parameters influence the onset location. To ensure that this bias is not the reason for the different ground B magnitudes, we further separate the onsets by the sign of IMF B_y and dipole tilt angle. Panels c,d,e and f of figure 1 show maps of ground B for early and late onsets with the different polarity of IMF B_y , and $|B_y| > 1$ nT. We used measurements of IMF B_y with a 1-minute resolution provided from the OMNI data set, time shifted to the bow shock. We use the median during the 20 minutes prior to the substorm onset. For both polarities of IMF B_y , the magnitude of ground B for early onset substorms is higher than the magnitude for late onset substorms. Panels (g),(h),(i) and (j) of figure 1 show maps of ground B for substorms that occurred at times with different dipole tilt angle Ψ (Laundal & Richmond, 2017). For both signs of the dipole tilt angle, the magnitude of ground B is higher for early substorms than late substorms. These figures show that the bias in B_y and Ψ is not the reason for the different B magnitudes in the two columns.

Motivated by our results showing profound differences in the ionospheric state before early and late substorm onsets, we have examined the relationship between substorm onset MLT and four different parameters: The AL index, the solar wind aberration angle, the dipole tilt angle, and IMF B_y . For all variables except for dipole tilt angle, we use the median value during the 60 min prior to onset. Figures 2a–d show the results of a regression analysis of MLT and each of these variables separately. In each panel, the regressor is divided into 10 bins with an equal number of observations, and the median onset MLT is shown in blue (red) for substorms observed in the northern (southern) hemisphere. The vertical bars represent the standard error of the median (see, e.g., Greene, 2008, page 878). The dashed lines represent regression models to be discussed in more detail below. Figure 2e shows the result of a multivariable regression analysis where all four parameters are combined and will be explained below.

Figure 2a shows the relationship between the onset MLT and the AL index. The purpose of analyzing the variation between onset MLT and the AL index is to quantify the effect that is observed in Figure 1, that stronger magnetic field perturbations prior to a substorm are associated with earlier onset MLTs. The AL (auroral lower) index measures the maximum strength of the westward electrojet from 12 magnetometers longitudinally distributed along the auroral oval, and is here taken as a proxy of geomagnetic activity. The x axis of Figure 2a represents a modified AL, AL^* , defined as $\max(AL) - AL$, where $\max(AL)$ is the maximum value of $AL = 7.85$ nT. This ensures that AL^* is always positive. We see from Figure 2a that the variation of substorm onset MLT as a function of AL is nonlinear. We therefore seek a regression model on the form $y = a - bAL^{\gamma}$, where y is the onset MLT and a , b , and γ are model parameters to be fitted. Since AL^* is positive, y will be real for all γ . The model parameters are estimated using nonlinear least squares, with all data points individually (not the median values). The resulting model parameters are $a = 25.7$ h, $b = 1.69$ h/nT, and $\gamma = 0.1$. The coefficient of determination is 0.049, which means that the model explains about 4.9% of the variation of the substorm onset MLT, roughly the same as IMF B_y based statistical models (see Østgaard et al., 2011, and below). In contrast to variation with IMF B_y , the variation with AL is in the same direction in both hemispheres.

Figure 2b shows the relationship between the aberration angle and the MLT of the substorm onset. The aberration angle α is the angle between the Sun-Earth line and the solar wind velocity as defined by Hones et al. (1986). We calculate the aberration an-

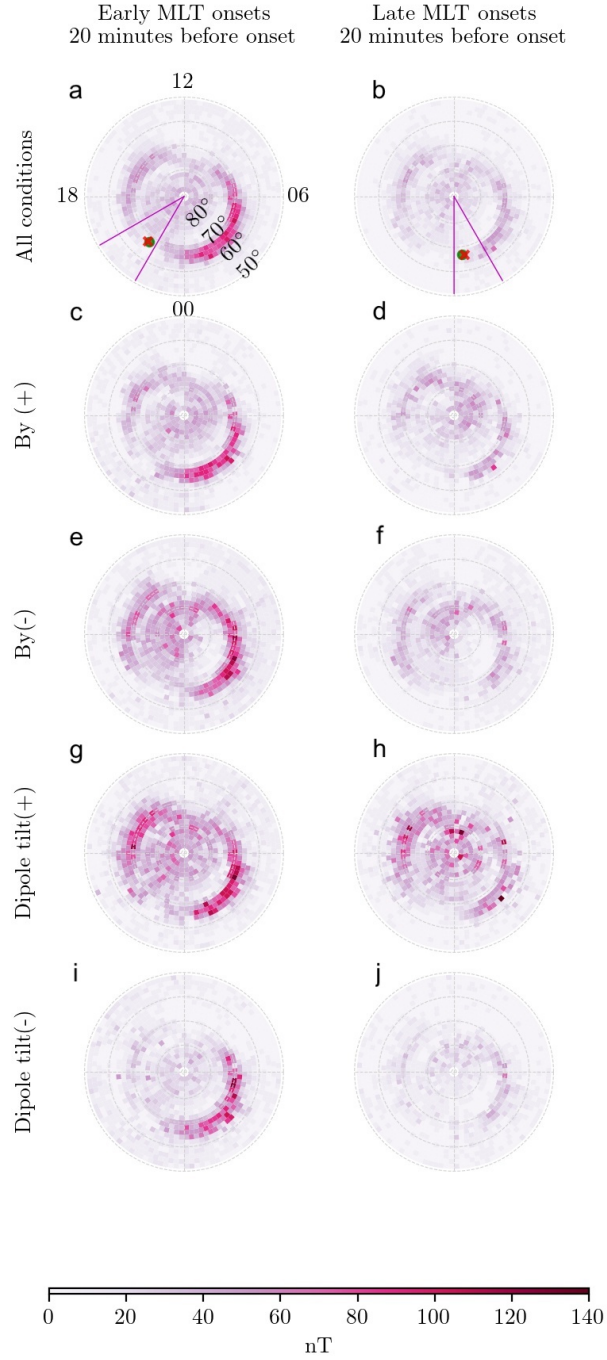


Figure 1. Maps of the magnitude of the average horizontal magnetic field perturbations (ground B) 20 minutes prior to the substorm onset. The left column shows onsets observed between 20 and 22 MLT (early) and the right column shows onsets observed between 24 and 02 MLT (late). Panels a and b show maps of early and late onsets based on all the available data. Panels c and d (e and f) show early and late onsets that occurred when IMF B_y was positive (negative). Panels g and h (i and j) show maps for positive (negative) dipole tilt angle. Each panel uses an equal-area grid with 2° MLAT resolution.

gle as $\alpha = \tan^{-1}(-V_y/V_x)$, where V_y is the solar wind velocity in the GSM y direction. The V_y provided by OMNI is given in an inertial frame, but we have converted to an Earth fixed frame by adding Earth's orbital speed, 29.8 km/s. We expect that the onset MLT varies linearly with aberration angle, since the magnetosphere aligns with the solar wind velocity (a "windsock effect"). This is also supported by the medians in Figure 2b. We therefore seek a model on the form $y = a + b\alpha$. We estimated model parameters are $a = 22.6$ h and $b = 0.96$, when the angle α is given in hours. The fact that b is so close to 1 is in agreement with the expected windsock effect. The coefficient of determination is 2.5%.

Figure 2c shows the relationship between the dipole tilt angle Ψ and the MLT of the substorm onset. We see that the onset MLT decreases (increases) with dipole tilt angle in the Northern (Southern) hemisphere. The figure indicates that the relationships are linear, so we seek models on the form $y_{n,s} = a_{n,s} + b_{n,s}\Psi$, where the subscripts refer to the Northern and Southern hemispheres. We find that $a_n(a_s) = 22.9(22.7)$ h and $b_n(b_s) = -0.006(0.002)$ h/degree. In both cases, the models explain less than 1% of the substorm onset MLT variation. However, since the number of samples is so large, the probability that this would occur by chance is less than 10^{-8} . In the other regression models, the correlation is higher, and the p -value is smaller.

Figure 2d shows the relationship between the IMF B_y component of the solar wind and the MLT of the substorm onset. S. E. Milan et al. (2010) suggested that for IMF B_y to impact the onset MLT, the polarity must be the same for a long time prior to the substorm onset. In our analysis, we used the average of IMF B_y one hour prior to the substorm onset. We see that if IMF B_y is negative (positive), the substorm onsets tend to be observed at later (earlier) local times in the northern (southern) hemisphere. For the opposite sign, the variation is minimal. This is in agreement with the results by Østgaard et al. (2011). Because of this, we seek regression models of the form

$$y_n = \begin{cases} a_n + b_n B_y & \text{if } B_y < 0 \\ a_n & \text{if } B_y \geq 0, \end{cases} \quad (1)$$

and for the southern hemisphere,

$$y_s = \begin{cases} a_s & \text{if } B_y < 0 \\ a_s + b_s B_y & \text{if } B_y \geq 0, \end{cases} \quad (2)$$

We find that $a_n(a_s) = 22.75(22.55)$ h, and $b_n(b_s) = 0.11(-0.10)$ h/nT. Both models explain about 4.5% of the variation in onset MLT.

Figure 2e shows the result of a multivariable regression analysis which includes all the above parameters. The multivariable model combines all the above model representations, and the model parameters are coestimated. In this model, we reverse the signs of B_y and dipole tilt angle Ψ for substorms observed in the Southern hemisphere. The resulting model is $y = 24.63 - 0.10B_y - 1.14AL^{*0.13} - 0.0035\Psi + 0.66\alpha$, where B_y and AL are given in nT, Ψ in degrees, and α in hours. Figure 2e shows each onset plotted against the model prediction as green dots. The dashed line represents where the data would be in the ideal case that the model makes perfect predictions. However, the model only captures 11.3% of the total variance of the MLT of the substorm onsets. The individual data points (green dots) are included in this panel to highlight the large degree of scatter. In the panels above, only binned medians are shown, although the individual data points were used in the regression analyses. The blue dots in Figure 2e also represent binned medians, in 10 bins based on model prediction quantiles, and we see that they follow the dashed line closely. The standard error of the median is too small to be noticed.

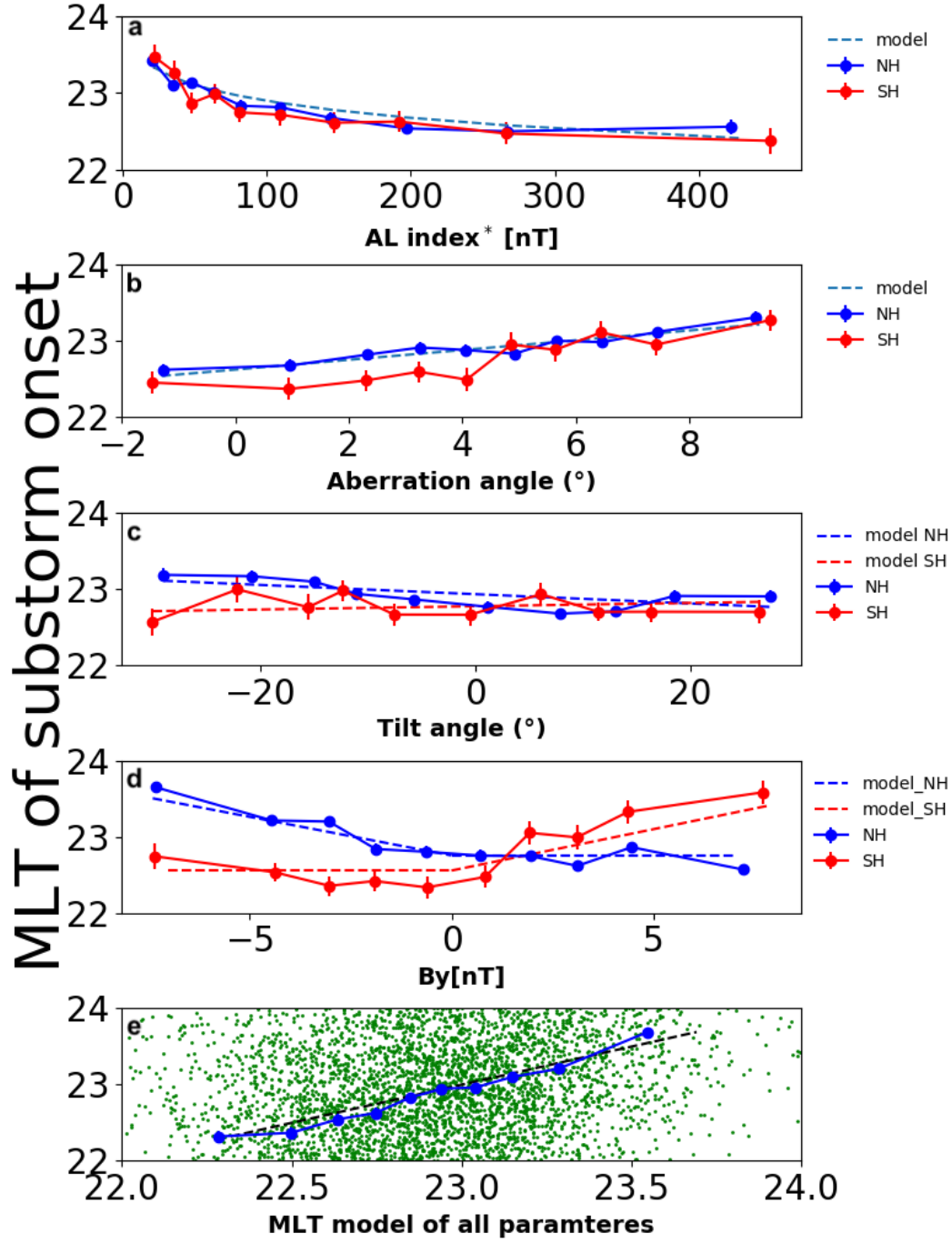


Figure 2. Figure 2 panels a,b,c,d shows the relationship between the substorm onset MLT and the AL index, the aberration angle, the dipole tilt angle and IMF B_y respectively, panel e shows the multivariable regression analysis with the four parameters. Each substorm onset from the combined lists is plotted against the model prediction as green dots. The black dashed line represents where the data would be in the ideal case that the model makes perfect predictions. Our model follow the dashed line closely.

3 Discussion and Summary

We have shown that substorm onsets tend to occur at earlier local times during geomagnetically active periods relative to substorm onsets during quiet periods. The regression analyses presented in Figures 2a and 2d show that the AL index prior to substorm onset is as strongly correlated with onset MLT as the IMF B_y , which has been reported in several earlier studies (Østgaard et al., 2011; Liou & Newell, 2010; Wang et al., 2007).

A key difference from the effect of IMF B_y is that the onset MLT dependence is the same in the two hemispheres with respect to AL. The effect of IMF B_y has been explained in terms of magnetic mapping: IMF B_y does not influence the location of the substorm onset in the magnetotail, only how it maps to the ionosphere, where we see the auroral emissions. The IMF B_y induces a B_y component in the magnetosphere with the same sign (Tenfjord et al., 2015), which causes the observed substorm onsets to shift in opposite directions in the two hemispheres. This mapping effect is illustrated in Figure 3a. The blue magnetic field line is symmetric between the two hemispheres, and the red magnetic field line illustrates what happens when we introduce a positive B_y in the magnetotail: The footpoint shifts towards dusk in the northern hemisphere and towards dawn in the southern hemisphere. Figure 3a.1 (a.2) shows the distribution of substorm onset locations observed in the northern (southern) hemisphere under B_y positive (green) and negative (orange) conditions. We see that the effect is in the opposite direction in the two hemispheres.

Figure 3b illustrates our interpretation of the onset MLT dependence on the AL index: Since the shift is in the same direction in both hemispheres, it is presumably not an effect of mapping, as with IMF B_y . Instead of a mapping effect, there is a real shift of substorm onset location in the magnetotail towards dusk when geomagnetic activity increases. The blue magnetic field line in Figure 3b represents a quiet time situation, and the red magnetic field line represents active times. Figure 3b.1 and Figure 3b.2) show the distribution of substorm onset locations observed in the northern hemisphere and the southern hemisphere respectively for high (green) and low (orange) activity, quantified in terms of the AL index prior to the substorm onset. We see that the effect is in the same direction in the two hemispheres.

The shift of substorm onsets towards dusk with increasing geomagnetic activity can be interpreted in terms of an electrostatic coupling between the magnetosphere and the ionosphere. McPherron (1991) discussed a clockwise rotation seen in the global Hall current pattern in terms of this electrostatic coupling (see their Figure 20). Due to lower conductivity in the polar cap relative to the auroral oval during active periods, a polarization electric field from midnight to noon adds to the dawn-dusk electric field, implying a shift towards dusk in the cross-polar cap flow and associated Hall currents. Presumably, this ionospheric feedback effect also leads to a shift towards dusk in magnetotail activity such as substorms. This was tested by Lotko et al. (2014) using a magnetohydrodynamic simulation of the magnetosphere, with an electrostatic coupling to the ionosphere. They performed three simulation runs using the same solar wind conditions, but three different high-latitude distributions of ionospheric conductance: First, uniform ionospheric conductance produced symmetric magnetotail activity with respect to the Sun-Earth line. Second, a realistic, empirical distribution with enhanced Hall conductance in the auroral oval produced magnetotail activity shifted towards dusk. Third, an unrealistic distribution of artificially depressed Hall conductance in the auroral oval produced magnetotail activity shifted toward dawn. These simulations clearly illustrate that ionospheric feedback can impact magnetosphere dynamics, and that it may explain the shift in substorm onset MLT reported here.

One issue that underlies the work of McPherron (1991) and Lotko et al. (2014) is that both rely on electrostatic models to represent the magnetosphere-ionosphere cou-

pling. In reality, the coupling is not electrostatic, and an electrostatic model cannot explain *how* ionospheric feedback causes magnetospheric activity to shift towards dusk. Determining the process by which ionospheric feedback regulates magnetospheric activity requires solving the equations that describe conservation of mass and momentum for ions and electrons moving through the neutral fluid, as they respond to electromagnetic fields that obey Maxwell's equations (e.g., Dreher, 1997).

Even though we have shown that the AL index is as useful in predictions of substorm onset MLT as IMF B_y , the explanatory power of our regression models (Figure 2) are all very low. A model that combines IMF B_y , the AL index, the aberration angle, and the dipole tilt angle explain about 11% of the observed variation in substorm onset MLT. The timing and location of substorm onsets therefore remain highly unpredictable.

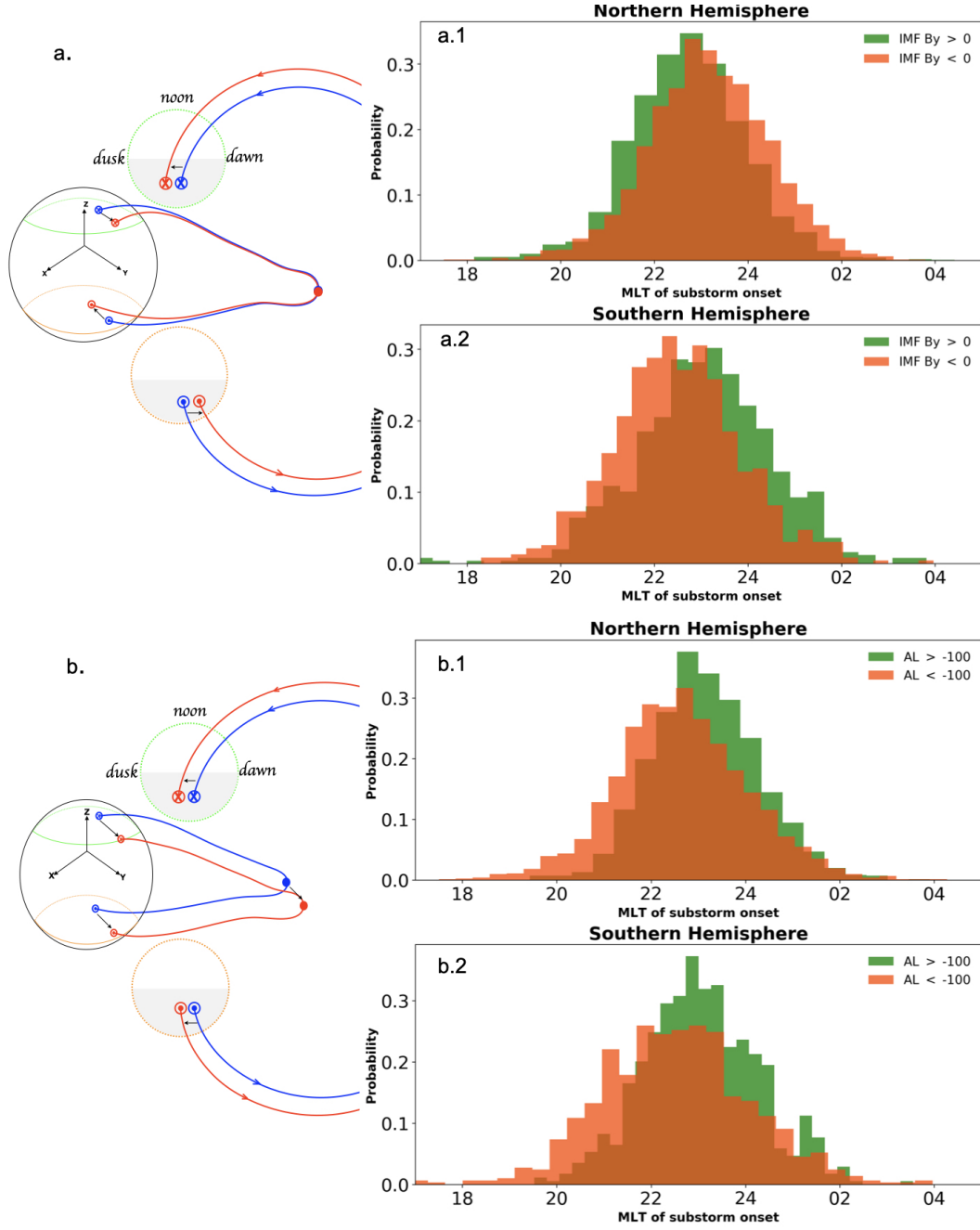


Figure 3. Conceptual figure illustrating a. the mapping effect and b. the real shift in the magnetotail. In panels a. and b., the green (orange) circle represent the northern (southern) hemisphere's high latitude ionosphere, the blue line is a magnetic field line to be shifted towards either dawn or dusk, appearing as the red line after the shift. The shift is in opposite direction between the northern and southern hemispheres in a and in the same direction in b. Panels a.1 and a.2 represents the distributions of the MLT of substorm onsets in Northern and Southern hemisphere respectively, the panels show that the the substorm onset MLT distribution observed in the northern (southern) hemisphere with positive IMF B_y shifts towards earlier (later) MLT. Panels b.1 and b.2 represents the distributions of the MLT of substorm onsets in Northern and Southern hemisphere respectively. The panels show that the substorm onset MLT observed in both northern and southern hemispheres shift towards earlier local time in both hemispheres for increased AL.

Acknowledgments

This study was supported by the Research Council of Norway/CoE under contracts 223252/F50 and 300844/F50, and by the Trond Mohn Foundation. For the ground magnetometer data we gratefully acknowledge: INTERMAGNET, Alan Thomson; CARISMA, PI Ian Mann; CANMOS, Geomagnetism Unit of the Geological Survey of Canada; The S-RAMP Database, PI K. Yumoto and Dr. K. Shiokawa; The SPIDR database; AARI, PI Oleg Troshichev; The MACCS program, PI M. Engebretson; GIMA; MEASURE, UCLA IGPP and Florida Institute of Technology; SAMBA, PI Eftyhia Zesta; 210 Chain, PI K. Yumoto; SAMNET, PI Farideh Honary; IMAGE, PI Liisa Juusola; Finnish Meteorological Institute, PI Liisa Juusola; Sodankylä Geophysical Observatory, PI Tero Raita; UiT the Arctic University of Norway, Tromsø Geophysical Observatory, PI Magnar G. Johnsen; GFZ German Research Centre For Geosciences, PI Jürgen Matzka; Institute of Geophysics, Polish Academy of Sciences, PI Anne Neska and Jan Reda; Polar Geophysical Institute, PI Alexander Yahnin and Yaroslav Sakharov; Geological Survey of Sweden, PI Gerhard Schwarz; Swedish Institute of Space Physics, PI Masatoshi Yamauchi; AUTUMN, PI Martin Connors; DTU Space, Thom Edwards and PI Anna Willer; South Pole and McMurdo Magnetometer, PI's Louis J. Lanzarotti and Alan T. Weatherwax; ICESTAR; RAPID-MAG; British Antarctic Survey; McMac, PI Dr. Peter Chi; BGS, PI Dr. Susan Macmillan; Pushkov Institute of Terrestrial Magnetism, Ionosphere and Radio Wave Propagation (IZMIRAN); MFGI, PI B. Heilig; Institute of Geophysics, Polish Academy of Sciences, PI Anne Neska and Jan Reda; University of L'Aquila, PI M. Vellante; BCMT, V. Lesur and A. Chambodut; Data obtained in cooperation with Geoscience Australia, PI Andrew Lewis; AALPIP, co-PIs Bob Clauer and Michael Hartinger; MagStar, PI Jennifer Gannon; SuperMAG, PI Jesper W. Gjerloev; Data obtained in cooperation with the Australian Bureau of Meteorology, PI Richard Marshall. We acknowledge as well the use of NASA/GSFC's Space Physics Data Facility's OMNIWeb service, and OMNI data.)

4 Data sharing

Magnetometer data can be downloaded directly from <https://supermag.jhuapl.edu/>
Solar wind data can be downloaded from <https://omniweb.gsfc.nasa.gov/>.

References

- Akasofu, S. I. (1964). The development of the auroral substorm. *Planetary and Space Science*, 12(4), 273–282. doi: 10.1016/0032-0633(64)90151-5
- Dreher, J. (1997). On the self-consistent description of dynamic magnetosphere-ionosphere coupling phenomena with resolved ionosphere. *J. Geophys. Res.*, 102, 85–94. doi: 10.1029/96JA02800
- Frey, H. U., Mende, S. B., Angelopoulos, V., & Donovan, E. F. (2004). Substorm onset observations by IMAGE-FUV. *Journal of Geophysical Research: Space Physics*, 109(A10), 2. doi: 10.1029/2004JA010607
- Gabrielse, C., Angelopoulos, V., Runov, A., & Turner, D. L. (2014). Statistical characteristics of particle injections throughout the equatorial magnetotail. *Journal of Geophysical Research: Space Physics*, 119(4), 2512–2535. Retrieved from <https://agupubs.onlinelibrary.wiley.com/doi/abs/10.1002/2013JA019638>
doi: <https://doi.org/10.1002/2013JA019638>
- Gérard, J. C., Hubert, B., Grard, A., Meurant, M., & Mende, S. B. (2004). Solar wind control of auroral substorm onset locations observed with the IMAGE-FUV imagers. *Journal of Geophysical Research: Space Physics*, 109(A3), 1–13. doi: 10.1029/2003JA010129
- Gjerloev, J. W. (2012). The SuperMAG data processing technique. *Journal of Geophysical Research: Space Physics*, 117(9), 1–19. doi: 10.1029/2012JA017683
- Greene, W. H. (2008). *gree50240_FM.tex*. Retrieved from papers2://publication/

- uuid/A7DA6A91-12FF-4E6A-943F-1B97FFD010C0
- Grocott, A., Laurens, H. J., & Wild, J. A. (2017). Nightside ionospheric convection asymmetries during the early substorm expansion phase: Relationship to onset local time. *Geophysical Research Letters*, 44(23), 11,696–11,705. Retrieved from <https://agupubs.onlinelibrary.wiley.com/doi/abs/10.1002/2017GL075763> doi: <https://doi.org/10.1002/2017GL075763>
- Hones, E. W., Zwickl, R. D., Fritz, T. A., & Bame, S. J. (1986). Structural and dynamical aspects of the distant magnetotail determined from ISEE-3 plasma measurements. *Planetary and Space Science*, 34(10), 889–901. doi: 10.1016/0032-0633(86)90001-2
- Laundal, K. M., & Richmond, A. D. (2017). Magnetic Coordinate Systems. *Space Science Reviews*, 206(1-4), 27–59. Retrieved from <http://dx.doi.org/10.1007/s11214-016-0275-y> doi: 10.1007/s11214-016-0275-y
- Liou, K. (2010). Polar Ultraviolet Imager observation of auroral breakup. *Journal of Geophysical Research: Space Physics*, 115(12), 1–7. doi: 10.1029/2010JA015578
- Liou, K., & Newell, P. T. (2010). On the azimuthal location of auroral breakup: Hemispheric asymmetry. *Geophysical Research Letters*, 37(23), 1–5. doi: 10.1029/2010GL045537
- Liou, K., Newell, P. T., Sibeck, D. G., Meng, C. I., Brittnacher, M., & Parks, G. (2001). Observation of IMF and seasonal effects in the location of auroral substorm onset. *Journal of Geophysical Research: Space Physics*, 106(4), 5799–5810. doi: 10.1029/2000ja003001
- Lotko, W., Smith, R. H., Zhang, B., Ouellette, J. E., Brambles, O. J., & Lyon, J. G. (2014). Ionospheric control of magnetotail reconnection. *Science*, 345(6193), 184–187. doi: 10.1126/science.1252907
- Lui, A. T. Y. (1991). A synthesis of magnetospheric substorm models. *Journal of Geophysical Research: Space Physics*, 96(A2), 1849–1856. Retrieved from <https://agupubs.onlinelibrary.wiley.com/doi/abs/10.1029/90JA02430> doi: <https://doi.org/10.1029/90JA02430>
- McPherron, R. L. (1970). Growth phase of magnetospheric substorms. *Journal of Geophysical Research*, 75(28), 5592–5599. doi: 10.1029/ja075i028p05592
- McPherron, R. L. (1991). *Physical Processes Producing Magnetospheric Substorms and Magnetic Storms* (Vol. 4). ACADEMIC PRESS LIMITED. Retrieved from <http://dx.doi.org/10.1016/B978-0-12-378674-6.50013-3> doi: 10.1016/B978-0-12-378674-6.50013-3
- McPherron, R. L., & Chu, X. (2016). Relation of the auroral substorm to the substorm current wedge. *Geoscience Letters*, 3(1). doi: 10.1186/s40562-016-0044-5
- Milan, Hutchinson, many, et al. (2009). Influences on the radius of the auroral oval.
- Milan, S. E., Grocott, A., & Hubert, B. (2010). A superposed epoch analysis of auroral evolution during substorms: Local time of onset region. *Journal of Geophysical Research: Space Physics*, 115(10), 1–9. doi: 10.1029/2010JA015663
- Østgaard, N., Laundal, K. M., Juusola, L., Åsnes, A., Håland, S. E., & Weygand, J. M. (2011). Interhemispherical asymmetry of substorm onset locations and the interplanetary magnetic field. *Geophysical Research Letters*, 38(8), 1–5. doi: 10.1029/2011GL046767
- Østgaard, N., Mende, S. B., Frey, H. U., Immel, T. J., Frank, L. A., Sigwarth, J. B., & Stubbs, T. J. (2004). Interplanetary magnetic field control of the location substorm onset and auroral features in the conjugate hemisphere. *J. Geophys. Res.*, 109. doi: 10.1029/2003JA010370
- Østgaard, N., Tsyganenko, N. A., Mende, S. B., Frey, H. U., Immel, T. J., Fillingim, M., ... Sigwarth, J. B. (2005). Observations and model predictions of substorm auroral asymmetries in the conjugate hemispheres. *Geophys. Res. Lett.*, 32. doi: 10.1029/2004GL022166
- Richmond, A. D. (1995). Ionospheric Electrodynamics Using Magnetic Apex Coordi-

- 367 nates. *Journal of geomagnetism and geoelectricity*, 47(2), 191–212. doi: 10.5636/
368 jgg.47.191
- 369 Tenfjord, P., Østgaard, N., Snekvik, K., Laundal, K. M., Reistad, J. P., Haaland, S.,
370 & Milan, S. E. (2015). How the IMF By induces a By component in the closed
371 magnetosphere and how it leads to asymmetric currents and convection patterns
372 in the two hemispheres. *Journal of Geophysical Research A: Space Physics*,
373 120(11), 9368–9384. doi: 10.1002/2015JA021579
- 374 Tsyganenko, N. A. (1998). Modeling of twisted/warped magnetospheric con-
375 figurations using the general deformation method. *Journal of Geophysical*
376 *Research: Space Physics*, 103(A10), 23551–23563. Retrieved from [https://](https://agupubs.onlinelibrary.wiley.com/doi/abs/10.1029/98JA02292)
377 agupubs.onlinelibrary.wiley.com/doi/abs/10.1029/98JA02292 doi:
378 <https://doi.org/10.1029/98JA02292>
- 379 Wang, H., Lüher, H., Ma, S. Y., & Frey, H. U. (2007). Interhemispheric comparison
380 of average substorm onset locations: Evidence for deviation from conjugacy. *An-*
381 *nales Geophysicae*, 25(4), 989–999. doi: 10.5194/angeo-25-989-2007

conceptual_figure.jpeg.

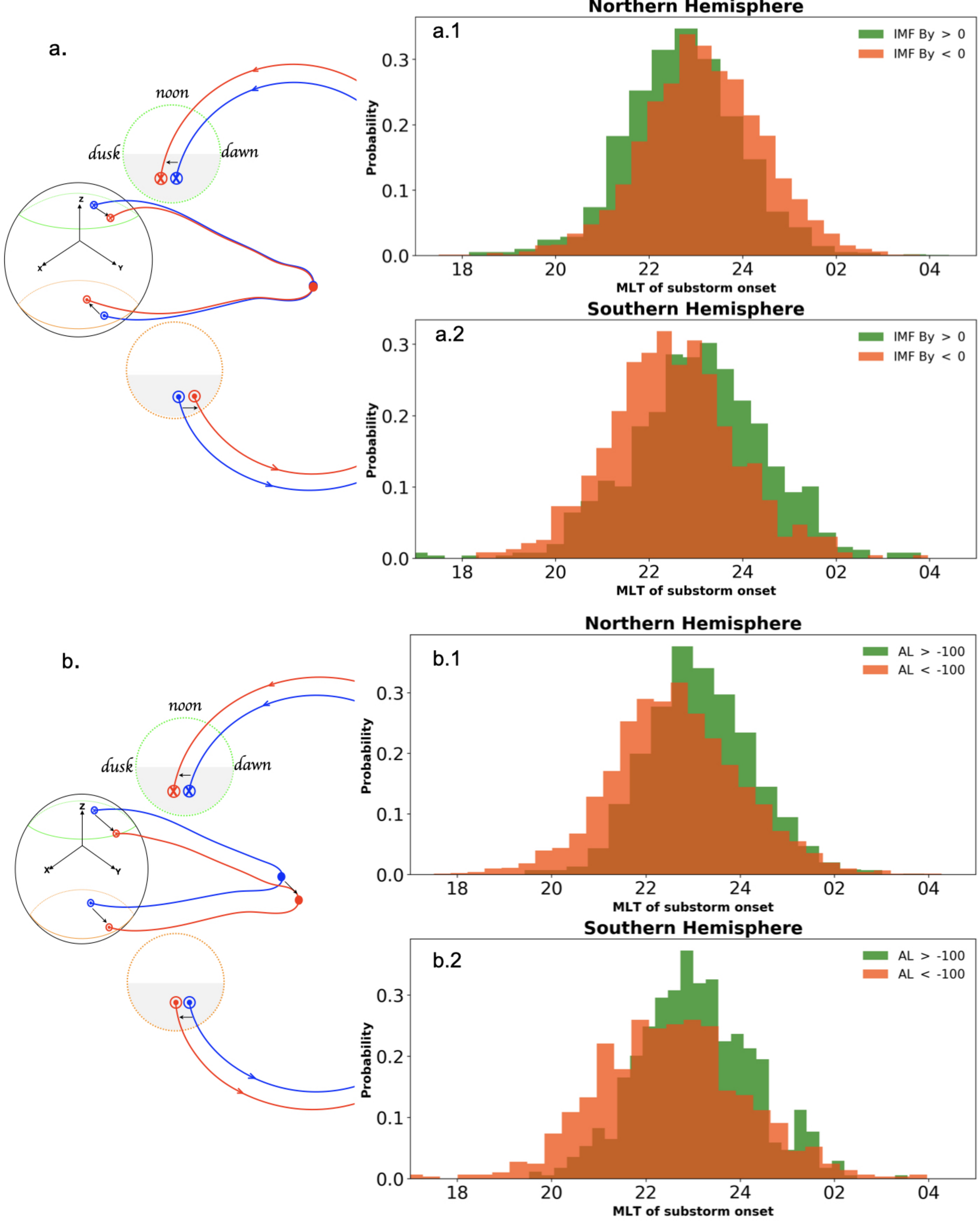


figure2.png.

MLT of substorm onset

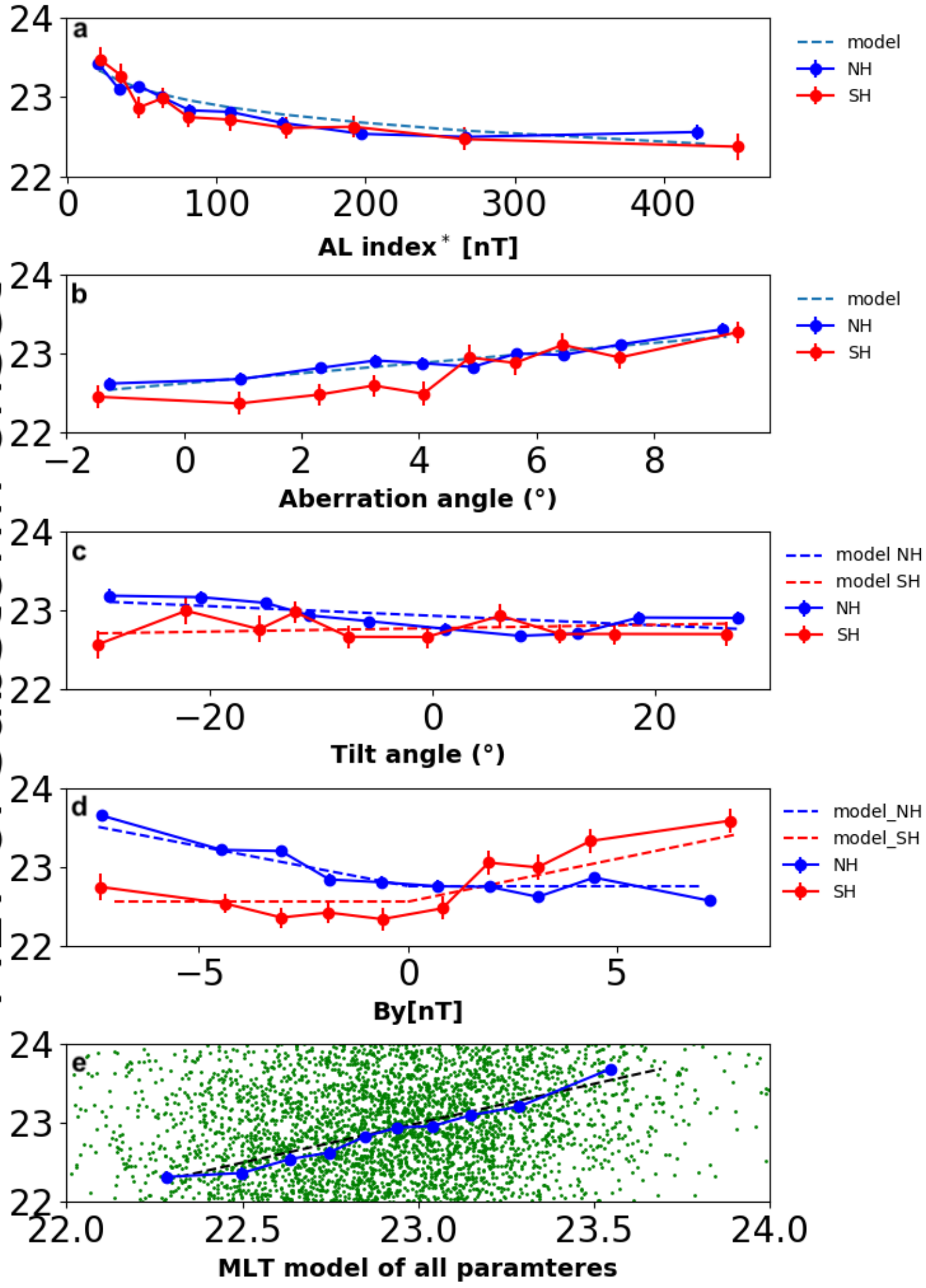
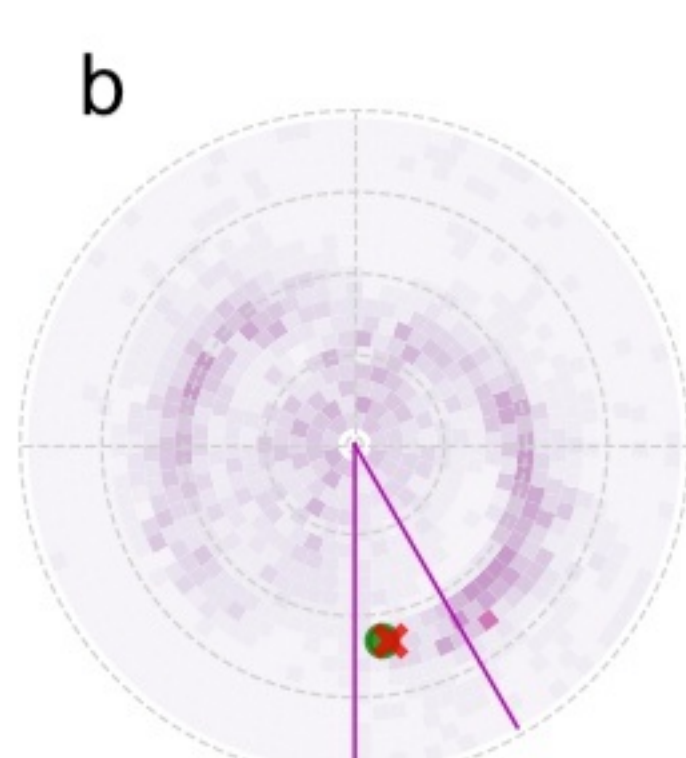
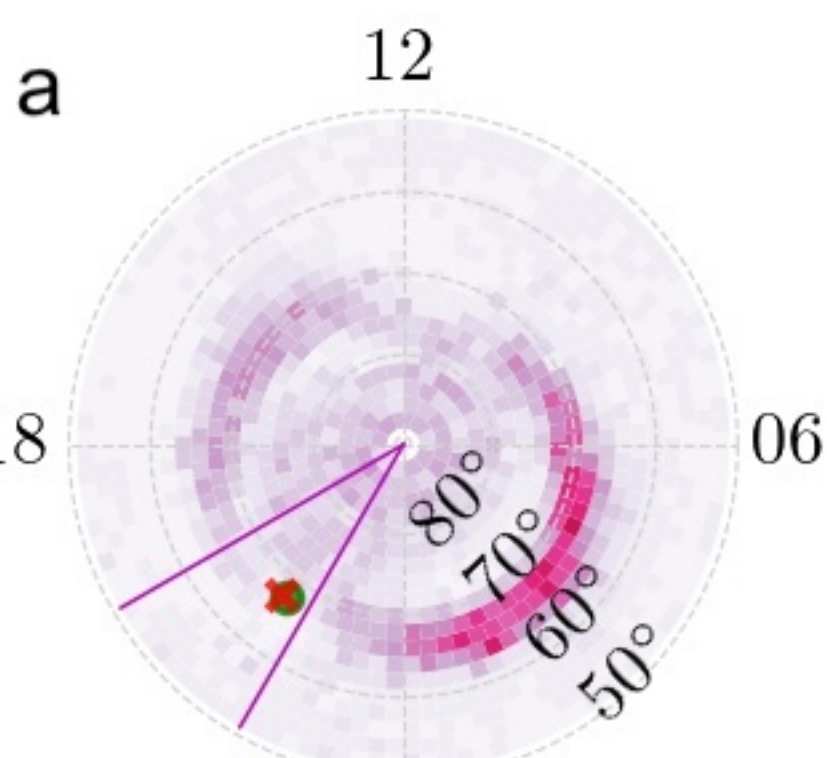


figure1.jpg.

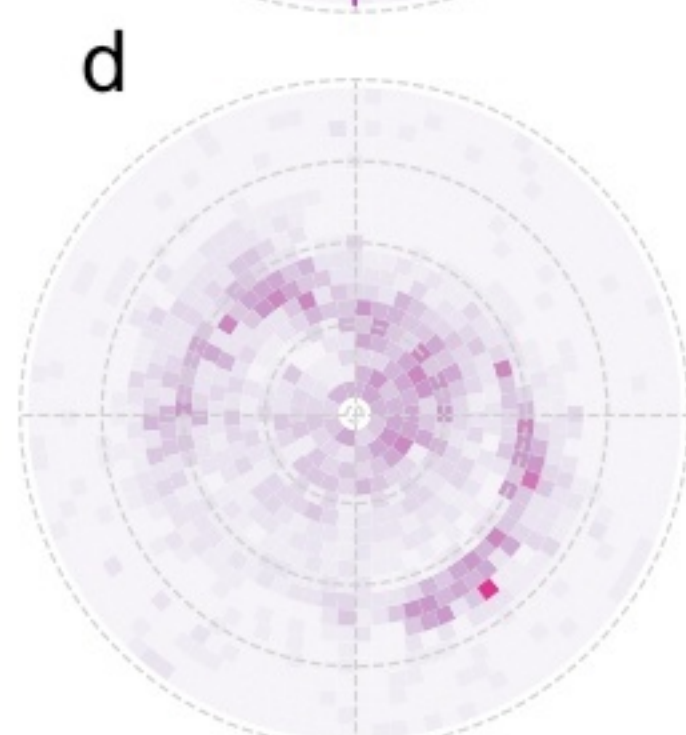
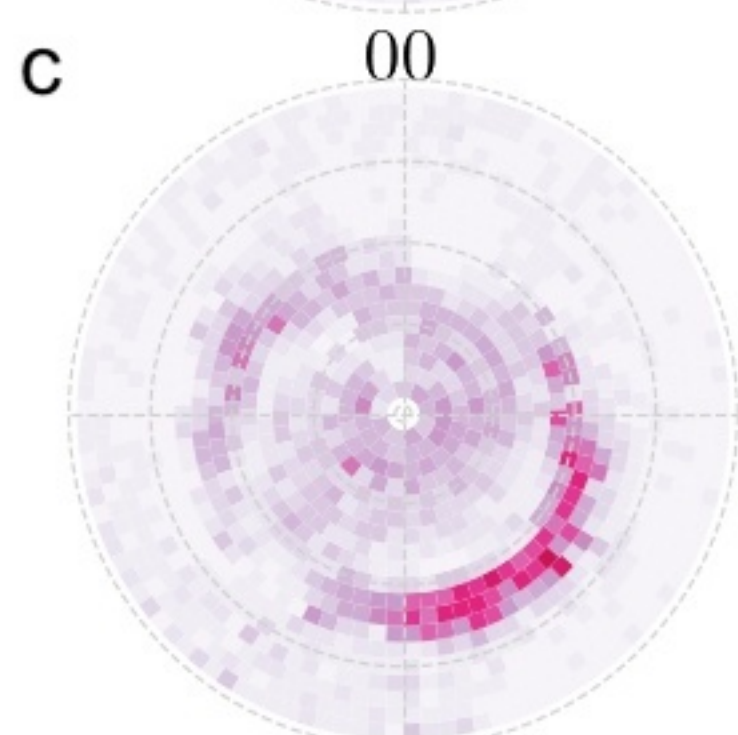
Early MLT onsets
20 minutes before onset

Late MLT onsets
20 minutes before onset

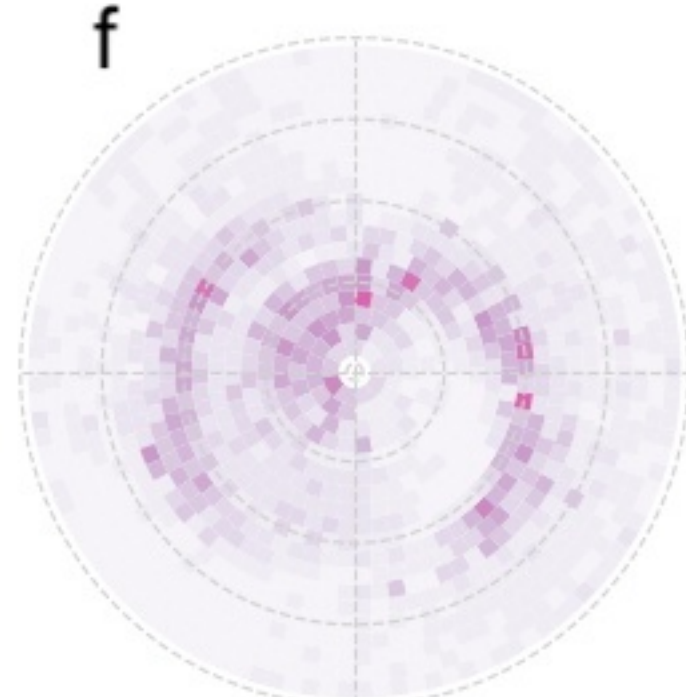
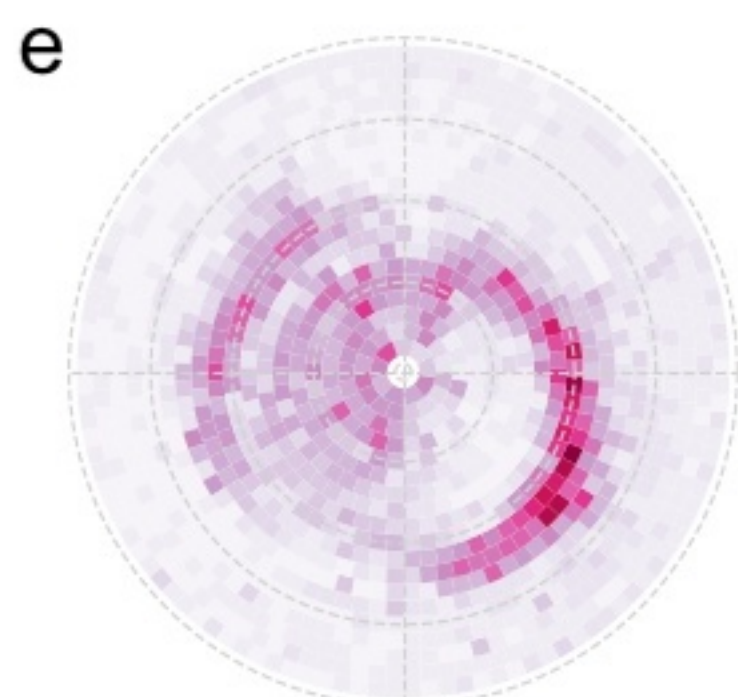
All conditions



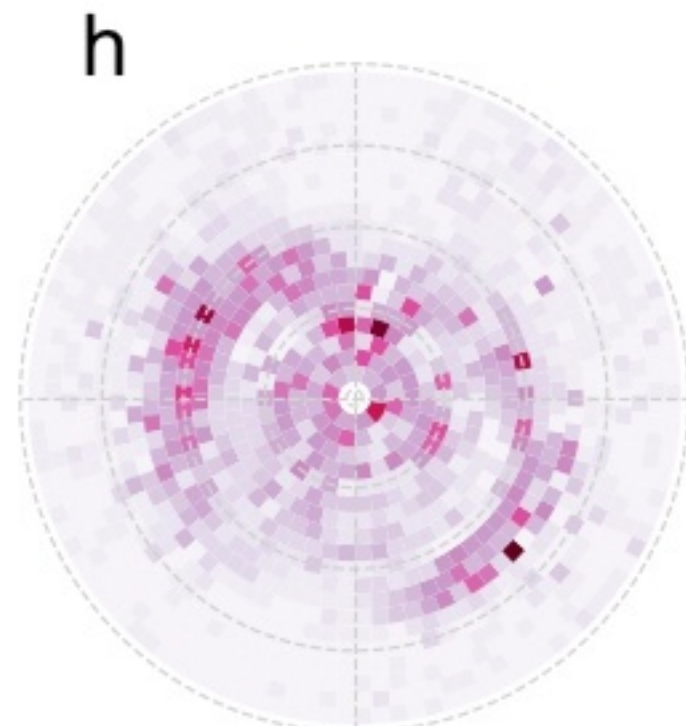
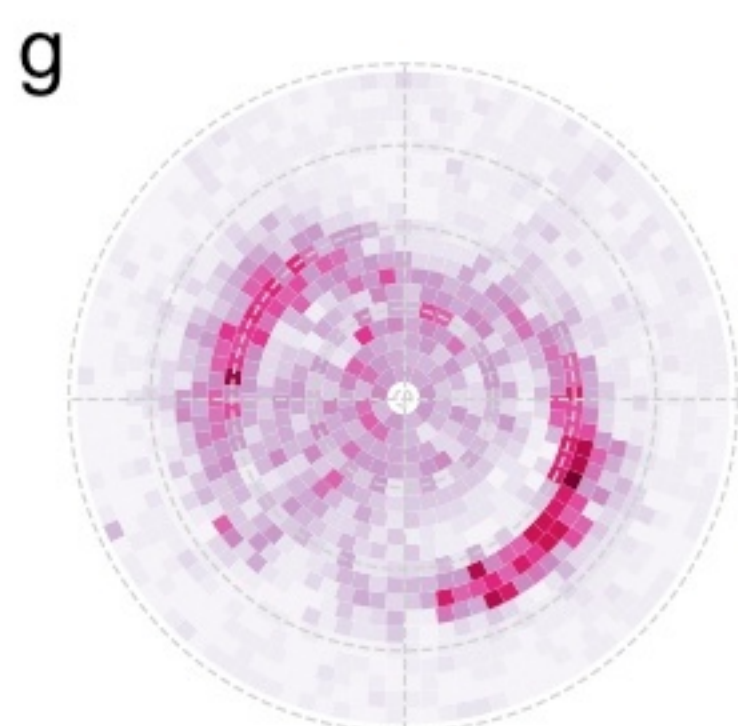
By (+)



By (-)



Dipole tilt(+)



Dipole tilt(-)

